Electronic Supplementary Material (ESI) for RSC Advances.

Supporting Information

MALDI-TOF MS and ESI-LTQ-Orbitrap tandem mass spectrometry reveal specific porphyranase activity from *Pseudoalteromonas atlantica* bacterial extract

C. Przybylski,[a b] G. Correc,[c] M. Fer,[c†] F. Gonnet,[a b] W. Helbert,[c†] Régis Daniel,[a b *]*

[a] CNRS, UMR 8587, Laboratoire Analyse et Modélisation pour la Biologie et l'Environnement, F-91025 Evry France

[b] Université Evry-Val-d'Essonne, Laboratoire Analyse et Modélisation pour la Biologie et l'Environnement, F-91025 Evry, France

[c] Université Pierre et Marie Curie, Paris VI, Végétaux Marins et Biomolécules, CNRS, UMR 7139, Station Biologique de Roscoff, 29680 Roscoff, France

[†]Present adress: Centre de Recherches sur les Macromolécules Végétales, Equipe Chimie et Biotechnologie des Oligosaccharide, UPR CNRS 5301, 38041 Grenoble Cedex, France.

Table S1. Oligosaccharides detected by MALDI-TOF MS in negative ionization mode after depolymerization of porphyran by a protein extract from the marine bacterium *Pseudoalteromonas atlantica* (only ions with intensity corresponding to ≥1% of the relative abundance are reported).

dp	m/z		Tentative assignment
	experimental	theoretical	
2	421.10	421.07	[(L6S–G)-Na]$^-$
	435.09	435.08	[(L6S–G)+CH_3-Na]$^-$
3	583.14	583.15	[(G)(L6S–G)-Na]$^-$
	597.15	597.13	[(G)(L6S–G)+CH_3-Na]$^-$
4	727.16	727.16	[(LA–G)(L6S–G)-Na]$^-$
	741.17	741.18	[(LA–G)(L6S–G)+CH_3-Na]$^-$
	745.17	745.17	[(L–G)(L6S–G)-Na]$^-$
	755.19	755.19	[(LA–G)(L6S–G)+2CH_3-Na]$^-$
	759.18	759.19	[(L–G)(L6S–G)+CH_3-Na]$^-$
	773.19	773.20	[(L–G)(L6S–G)+2CH_3-Na]$^-$
	847.11	847.11	[$(L6S–G)_2$-Na]$^-$
	861.12	861.13	[$(L6S–G)_2$+CH_3-Na]$^-$
	875.13	875.14	[$(L6S–G)_2$+2CH_3-Na]$^-$
	877.12	877.10	[$(L6S–G)_2$+CH_3-2Na+K]$^-$
5	889.20	889.21	[(G)(LA–G)(L6S–G)-Na]$^-$
	903.23	903.23	[(G)(LA–G)(L6S–G)+CH_3-Na]$^-$
	917.24	917.24	[(G)(LA–G)(L6S–G)+2CH_3-Na]$^-$
	921.24	921.24	[(G)(L–G)(L6S–G)+CH_3-Na]$^-$
	935.25	935.25	[(G)(L–G)(L6S–G)+2CH_3-Na]$^-$
	991.17	991.15	[(LA)$(L6S–G)_2$-Na]$^-$
	1005.17	1005.17	[(LA)$(L6S–G)_2$+CH_3-Na]$^-$
	1009.16	1009.16	[(G)$(L6S–G)_2$-Na]$^-$
	1023.17	1023.18	[(G)$(L6S–G)_2$+CH_3-Na]$^-$
	1037.19	1037.19	[(G)$(L6S–G)_2$+2CH_3-Na]$^-$
6	1033.25	1033.26	[$(LA–G)_2$(L6S–G)-Na]$^-$
	1047.25	1047.27	[$(LA–G)_2$(L6S–G)+CH_3-Na]$^-$
	1051.30	1051.31	[(LA–G)(L–G)(L6S–G)-Na]$^-$
	1061.28	1061.29	[$(LA–G)_2$(L6S–G)+2CH_3-Na]$^-$
	1065.26	1065.28	[(LA–G)(L–G)(L6S–G)+CH_3-Na]$^-$
	1069.26	1069.28	[$(L–G)_2$(L6S–G)-Na]$^-$
	1079.29	1079.30	[(LA–G)(L–G)(L6S–G)+2CH_3-Na]$^-$
	1083.27	1083.29	[$(L–G)_2$(L6S–G)+CH_3-Na]$^-$
	1093.29	1093.31	[(LA–G)(L–G)(L6S–G)+3CH_3-Na]$^-$
	1097.29	1097.31	[$(L–G)_2$(L6S–G)+2CH_3-Na]$^-$
	1111.30	1111.32	[$(L–G)_2$(L6S–G)+3CH_3-Na]$^-$
	1153.19	1153.20	[(LA–G)$(L6S–G)_2$-Na]$^-$
	1167.20	1167.22	[(LA–G)$(L6S–G)_2$+CH_3-Na]$^-$
	1171.21	1171.22	[(L–G)$(L6S–G)_2$-Na]$^-$
	1181.23	1181.24	[(LA–G)$(L6S–G)_2$+2CH_3-Na]$^-$
	1185.21	1185.23	[(L–G)$(L6S–G)_2$+CH_3-Na]$^-$
	1195.23	1195.25	[(LA–G)$(L6S–G)_2$+3CH_3-Na]$^-$
	1199.23	1199.25	[(L–G)$(L6S–G)_2$+2CH_3-Na]$^-$
	1213.27	1213.26	[(L–G)$(L6S–G)_2$+3CH_3-Na]$^-$
	1273.16	1273.15	[$(L6S–G)_3$-Na]$^-$
	1287.15	1287.17	[$(L6S–G)_3$+CH_3-Na]$^-$
	1301.17	1301.19	[$(L6S–G)_3$+2CH_3-Na]$^-$
	1315.18	1315.20	[$(L6S–G)_3$+3CH_3-Na]$^-$

Table S1. *Continued*

dp	m/z		Tentative assignment
	experimental	theoretical	
	1317.15	1317.16	$[(L6S–G)_3+2CH_3-2Na+K]^-$
6	1331.20	1331.17	$[(L6S–G)_3+3CH_3-2Na+K]^-$
	1333.12	1333.13	$[(L6S–G)_3+2CH_3-3Na+2K]^-$
	1227.30	1227.33	$[(G)(LA–G)(L–G)(L6S–G)+CH_3-Na]^-$
	1241.33	1241.35	$[(G)(LA–G)(L–G)(L6S–G)+2CH_3-Na]^-$
	1255.34	1255.37	$[(G)(LA–G)(L–G)(L6S–G)+3CH_3-Na]^-$
7	1269.34	1269.38	$[(G)(LA–G)(L–G)(L6S–G)+4CH_3-Na]^-$
	1329.24	1329.27	$[(G)(LA–G)(L6S–G)_2+CH_3-Na]^-$
	1343.27	1343.29	$[(G)(LA–G)(L6S–G)_2+2CH_3-Na]^-$
	1361.27	1361.30	$[(G)(L–G)(L6S–G)_2+2CH_3-Na]^-$
	1357.34	1357.36	$[(LA–G)_2(L–G)(L6S–G)-Na]^-$
	1371.37	1371.38	$[(LA–G)_2(L–G)(L6S–G)+CH_3-Na]^-$
	1375.35	1375.37	$[(LA–G)(L–G)_2(L6S–G)-Na]^-$
	1385.40	1385.39	$[(LA–G)_2(L–G)(L6S–G)+2CH_3-Na]^-$
	1389.37	1389.39	$[(LA–G)(L–G)_2(L6S–G)+CH_3-Na]^-$
	1393.36	1393.38	$[(L–G)_3(L6S–G)-Na]^-$
	1399.40	1399.41	$[(LA–G)_2(L–G)(L6S–G)+3CH_3-Na]^-$
	1403.38	1403.40	$[(LA–G)(L–G)_2(L6S–G)+2CH_3-Na]^-$
	1407.39	1407.40	$[(L–G)_3(L6S–G)+CH_3-Na]^-$
	1417.40	1417.42	$[(LA–G)(L–G)_2(L6S–G)+3CH_3-Na]^-$
	1421.40	1421.41	$[(L–G)_3(L6S–G)+2CH_3-Na]^-$
	1431.42	1431.43	$[(LA–G)(L–G)_2(L6S–G)+4CH_3-Na]^-$
	1435.42	1435.43	$[(L–G)_3(L6S–G)+3CH_3-Na]^-$
	1459.29	1459.30	$[(LA–G)_2(L6S–G)_2-Na]^-$
	1473.30	1473.32	$[(LA–G)_2(L6S–G)_2+CH_3-Na]^-$
	1475.25	1475.27	$[(LA–G)_2(L6S–G)_2-2Na+K]^-$
	1477.29	1477.31	$[(LA–G)(L–G)(L6S–G)_2-Na]^-$
	1487.31	1487.33	$[(LA–G)_2(L6S–G)_2+2CH_3-Na]^-$
	1489.27	1489.29	$[(LA–G)_2(L6S–G)_2+CH_3-2Na+K]^-$
	1491.32	1491.33	$[(LA–G)(L–G)(L6S–G)_2+CH_3-Na]^-$
8	1503.30	1503.31	$[(LA–G)_2(L6S–G)_2+2CH_3-2Na+K]^-$
	1505.32	1505.34	$[(LA–G)(L–G)(L6S–G)_2+2CH_3-Na]^-$
	1509.33	1509.34	$[(L–G)_2(L6S–G)_2+CH_3-Na]^-$
	1519.35	1519.36	$[(LA–G)(L–G)(L6S–G)_2+3CH_3-Na]^-$
	1521.30	1521.32	$[(LA–G)(L–G)(L6S–G)_2+2CH_3-2Na+K]^-$
	1523.34	1523.35	$[(L–G)_2(L6S–G)_2+2CH_3-Na]^-$
	1533.35	1533.37	$[(LA–G)(L–G)(L6S–G)_2+4CH_3-Na]^-$
	1537.36	1537.37	$[(L–G)_2(L6S–G)_2+3CH_3-Na]^-$
	1551.36	1551.38	$[(L–G)_2(L6S–G)_2+4CH_3-Na]^-$
	1579.27	1579.25	$[(LA–G)(L6S–G)_3-Na]^-$
	1593.25	1593.26	$[(LA–G)(L6S–G)_3+CH_3-Na]^-$
	1597.25	1597.26	$[(L–G)(L6S–G)_3-Na]^-$
	1607.30	1607.28	$[(LA–G)(L6S–G)_3+2CH_3-Na]^-$
	1611.26	1611.28	$[(L–G)(L6S–G)_3+CH_3-Na]^-$
	1621.31	1621.30	$[(LA–G)(L6S–G)_3+3CH_3-Na]^-$
	1625.28	1625.29	$[(L–G)(L6S–G)_3+2CH_3-Na]^-$
	1635.33	1635.31	$[(LA–G)(L6S–G)_3+4CH_3-Na]^-$
	1639.28	1639.31	$[(L–G)(L6S–G)_3+3CH_3-Na]^-$
	1653.30	1653.32	$[(L–G)(L6S–G)_3+4CH_3-Na]^-$
	1727.23	1727.23	$[(L–G)(L6S–G)_3+2CH_3-Na]^-$
	1741.23	1741.25	$[(L–G)(L6S–G)_3+3CH_3-Na]^-$
	1755.26	1755.28	$[(L–G)(L6S–G)_3+3CH_3-2Na+K]^-$

Table S1. *Continued*

dp	m/z		Tentative assignment
	experimental	theoretical	
8	1759.51	1759.53	$[(L–G)_4(L6S–G)+3CH_3-Na]^-$
	1783.40	1783.41	$[(LA–G)_2(L–G)(L6S–G)_2-Na]^-$
10	1795.32	1795.38	$[(LA–G)_3(L6S–G)_2+CH_3-2Na+K]^+$
	1797.41	1797.42	$[(LA–G)_2(L–G)(L6S–G)_2+CH_3-Na]^-$
	1801.41	1801.42	$[(LA–G)(L–G)_2(L6S–G)_2-Na]^-$
	1811.44	1811.44	$[(LA–G)_2(L–G)(L6S–G)_2+2CH_3-Na]^-$
	1815.43	1815.43	$[(LA–G)(L–G)_2(L6S–G)_2+CH_3-Na]^-$
	1819.42	1819.43	$[(L–G)_3(L6S–G)_2-Na]^-$
	1825.43	1825.45	$[(LA–G)_2(L–G)(L6S–G)_2+3CH_3-Na]^-$
	1829.43	1829.45	$[(LA–G)(L–G)_2(L6S–G)_2+2CH_3-Na]^-$
	1833.42	1833.44	$[(L–G)_3(L6S–G)_2+CH_3-Na]^-$
	1843.45	1843.46	$[(LA–G)(L–G)_2(L6S–G)_2+3CH_3-Na]^-$
	1847.44	1847.46	$[(L–G)_3(L6S–G)_2+2CH_3-Na]^-$
	1857.47	1857.48	$[(LA–G)(L–G)_2(L6S–G)_2+4CH_3-Na]^-$
	1861.46	1861.47	$[(L–G)_3(L6S–G)_2+3CH_3-Na]^-$
	1899.36	1899.36	$[(LA–G)_2(L6S–G)_3+CH_3-Na]^-$
	1913.36	1913.38	$[(LA–G)_2(L6S–G)_3+2CH_3-Na]^-$
	1917.35	1917.37	$[(LA–G)(L–G)(L6S–G)_3+CH_3-Na]^-$
	1931.37	1931.39	$[(LA–G)(L–G)(L6S–G)_3+2CH_3-Na]^-$
	1945.37	1945.40	$[(LA–G)(L–G)(L6S–G)_3+3CH_3-Na]^-$
	1949.37	1949.40	$[(L–G)_2(L6S–G)_3+2CH_3-Na]^-$
	1959.40	1959.42	$[(LA–G)(L–G)(L6S–G)_3+4CH_3-Na]^-$
	1963.37	1963.41	$[(L–G)_2(L6S–G)_3+3CH_3-Na]^-$
	2005.33	2005.29	$[(LA–G)(L6S–G)_4+CH_3-Na]^-$
	2019.35	2019.31	$[(LA–G)(L6S–G)_4+CH_3-Na]^-$
	2033.35	2033.32	$[(LA–G)(L6S–G)_4+2CH_3-Na]^-$
	2037.35	2037.32	$[(L–G)(L6S–G)_4+CH_3-Na]^-$
	2047.37	2047.34	$[(LA–G)(L6S–G)_4+3CH_3-Na]^-$
	2051.39	2051.34	$[(L–G)(L6S–G)_4+2CH_3-Na]^-$
	2061.38	2061.36	$[(LA–G)(L6S–G)_4+4CH_3-Na]^-$
	2065.37	2065.35	$[(L–G)(L6S–G)_4+3CH_3-Na]^-$
	2079.39	2079.37	$[(L–G)(L6S–G)_4+4CH_3-Na]^-$
	2139.29	2139.26	$[(L6S–G)_5+CH_3-Na]^-$
	2153.27	2153.27	$[(L6S–G)_5+2CH_3-Na]^-$
	2167.28	2167.29	$[(L6S–G)_5+3CH_3-Na]^-$
	2181.33	2181.31	$[(L6S–G)_5+4CH_3-Na]^-$
12	2107.52	2107.51	$[(LA–G)_2(L–G)_2(L6S–G)_2-Na]^-$
	2121.50	2121.53	$[(LA–G)_2(L–G)_2(L6S–G)_2+CH_3-Na]^-$
	2135.56	2135.54	$[(LA–G)_2(L–G)_2(L6S–G)_2+2CH_3-Na]^-$
	2149.53	2149.56	$[(LA–G)_2(L–G)_2(L6S–G)_2+3CH_3-Na]^-$
	2163.55	2163.57	$[(LA–G)_2(L–G)_2(L6S–G)_2+4CH_3-Na]^-$
	2237.51	223748	$[(LA–G)_2(L–G)(L6S–G)_3+2CH_3-Na]^-$
	2241.50	2241.48	$[(LA–G)\ (L–G)_2(L6S–G)_3+2CH_3-Na]^-$
	2251.53	2251.50	$[(LA–G)_2(L–G)(L6S–G)_3+3CH_3-Na]^-$
	2255.52	2255.49	$[(LA–G)\ (L–G)_2(L6S–G)_3+2CH_3-Na]^-$
	2259.52	2259.49	$[(L–G)_3(L6S–G)_3+2CH_3-Na]^-$
	2269.49	2269.51	$[(LA–G)(L–G)_2(L6S–G)_3+3CH_3-Na]^-$
	2283.49	2283.52	$[(LA–G)(L–G)_2(L6S–G)_3+4CH_3-Na]^-$
	2343.44	2343.41	$[(LA–G)(L–G)(L6S–G)_4+1CH_3-Na]^-$
	2357.47	2357.43	$[(LA–G)(L–G)(L6S–G)_4+2CH_3-Na]^-$
	2371.48	2371.45	$[(LA–G)(L–G)(L6S–G)_4+3CH_3-Na]^-$
	2385.46	2385.46	$[(LA–G)(L–G)(L6S–G)_4+4CH_3-Na]^-$

Table S1. *Continued*

dp	m/z	Tentative assignment

	experimental	theoretical	
12	2389.48	2389.46	$[(L–G)_2(L6S–G)_4+3CH_3\text{-}Na]^-$
	2445.35	2445.35	$[(LA–G)(L6S–G)_5+1CH_3\text{-}Na]^-$
	2459.38	2459.37	$[(LA–G)(L6S–G)_5+2CH_3\text{-}Na]^-$
	2473.40	2473.38	$[(LA–G)(L6S–G)_5+3CH_3\text{-}Na]^-$
	2487.42	2487.40	$[(LA–G)(L6S–G)_5+4CH_3\text{-}Na]^-$
	2491.41	2491.40	$[(L–G)(L6S–G)_5+3CH_3\text{-}Na]^-$
14	2561.60	2561.59	$[(LA–G)_2(L–G)_2(L6S–G)_3+2CH_3\text{-}Na]^-$
	2575.60	2575.60	$[(LA–G)_2(L–G)_2(L6S–G)_3+3CH_3\text{-}Na]^-$
	2681.53	2681.54	$[(LA–G)(L–G)_2(L6S–G)_4+2CH_3\text{-}Na]^-$
	2695.52	2695.55	$[(LA–G)(L–G)_2(L6S–G)_4+3CH_3\text{-}Na]^-$
	2815.47	2815.50	$[(L–G)_2(L6S–G)_5+3CH_3\text{-}Na]^-$

Text S1. MALDI-TOF reflector MS analysis of porphyran oligosaccharides produced by β-porphyranase A.

Crude porphyran (≈ 50 $kg.mol^{-1}$) from *P. umbilicalis* red algae was submitted to depolymerization by the purified enzyme β-porphyranase A, and subsequent size fractionation chromatography (SEC). The highest chromatographic resolution has been sought thanks to the use of three SEC columns in series. The resulting chromatogram exhibited a distribution of discrete peaks that could be attributed to di-, tetra- and hexasaccharides (dp2, dp4 and dp6, respectively) according to chromatographic standards.[1] This attribution was ascertained by MALDI-TOF analysis of the SEC fractions using the HABA/TMG_2 ionic liquid as a matrix well adapted to the MS analysis of sulfated oligosaccharides, in negative mode (See Materials and Methods section for details).[2-4] MALDI-TOF spectrum of the disaccharide fraction (dp2) revealed an unique and dominant ion at m/z 421.10 (Figure S1A; Table S2) in good agreement with theoretical m/z value (421.07) expected for a monosulfated dp2.

It is worth noting that the tetra- and hexasaccharide peaks on SEC chromatogram appeared as multi-component fractions. Consequently, the dp4 SEC fraction was analyzed by MALDI-TOF MS as two distinct sub-fractions, both containing di- and monosulfated tetrasaccharides, mainly under non-methylated form (at *m/z* 745.17 and 847.11, respectively) for one sub-fraction (Figure S1B; Table S2), and as monomethylated tetrasaccharide form (at *m/z* 759.19 and 861.14, respectively) for the other (Figure S1C; Table S2). The detection of the monomethylated species (at *m/z* 759.19 and *m/z* 861.14) in the former sub-fraction may be due to partial co-elution with non-methylated ones. Minor species arising from the Na^+/K^+ exchange were observed exclusively for the disulfated tetrasaccharides at *m/z* 863.08 (from *m/z* 847.11) and 877.10/877.11 (from *m/z* 861.14/861.13) (Figure S1B-C; Table S2). Other minor ions at *m/z* 583.15 and 597.13 (+ CH_3) were attributed to odd dp monosulfated trisaccharides arising likely from fragmentation during sample treatment. Some additional ions at m/z 1033.25, 1051.32 and 1153.22 (Figure S1B; Table S2), were tentatively attributed to hexasaccharides with 2 anhydrohexoses and 1 sulfate group, 1 anhydrohexose and 1 sulfate group, and 1

anhydrohexose and 2 sulfate groups, respectively, indicating that some co-eluted dp6 contaminated the dp4 fraction.

The dp6 SEC fraction was analyzed by MALDI-TOF reflector MS in negative mode as also two distinct sub-fractions, both containing di- and monosulfated hexasaccharides that included one anhydro-hexose residue (LA) (Figure S1D). The dp6 sub-fractions were differentiated by their methyl group content. One sub-fraction contained mainly non-methylated di- and monosulfated hexasaccharides (at *m/z* 1153.20 and 1051.31, respectively) with still minor species corresponding to their methylated counterparts (at *m/z* 1167.22 and 1065.28) (Figure S1D; Table S2), whereas the mono- and dimethylated sulfated hexasaccharides were the major species of the second sub-fraction (at *m/z* 1167.22 and 1065.28) (Figure S1E; Table S2). Finally, the mass spectrum (Figure S1E; Table S2), exhibited minor ions at *m/z* 1303.14 and 1317.18 that are in agreement with a fully sulfated (trisulfated) porphyran hexasaccharide without anhydrogalactose but with 1 or 2 methyl groups, respectively with both a Na^+/K^+ exchange. Other minor ions at *m/z* 1357.34 or m/z 1459.32 may be assigned to octasaccharides with 2 anhydrohexoses and 1 or 2 sulfate groups, respectively, indicating again some contamination by co-elution of higher dp species.

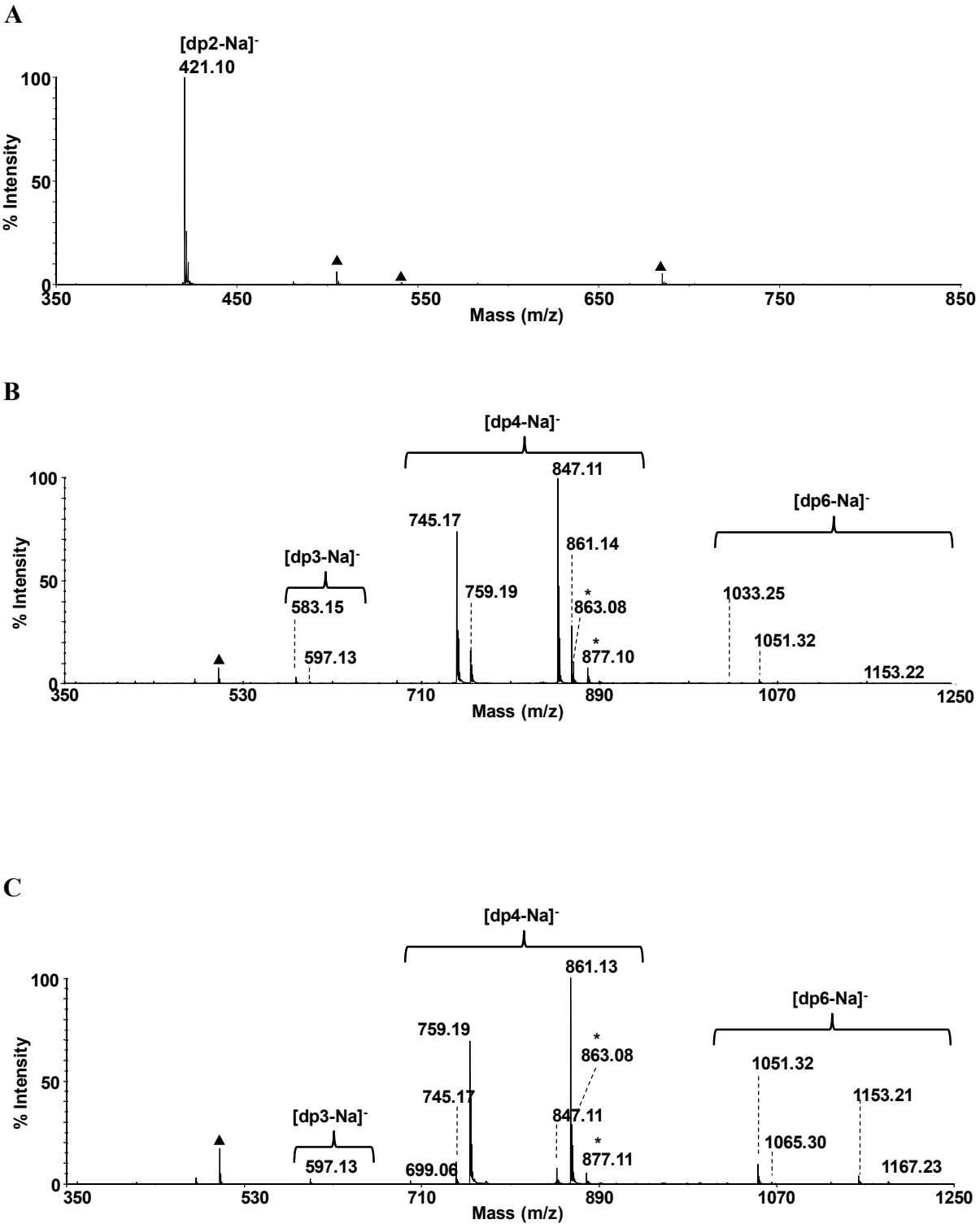

Figure S1. Negative ion reflector MALDI-TOF mass spectra of oligosaccharide SEC fractions after porphyran depolymerization by β-porphyranase A. Asterisks and diamonds represent potassium adducts and matrix adducts, respectively. Fractions of (A) dp2, (B) dp4, (C) dp4-Me, (D) dp6 and (E) dp6-Me.

D

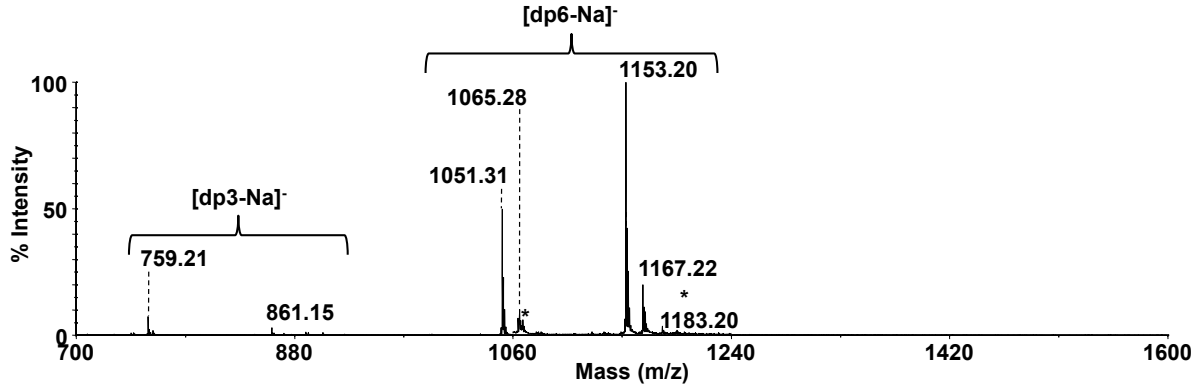

E

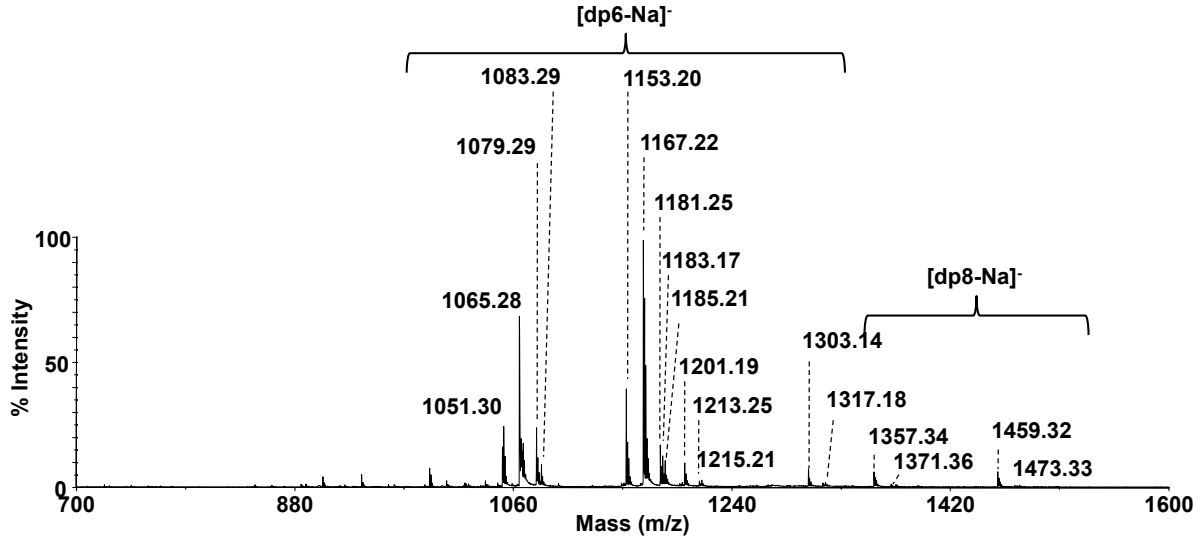

Figure S1. *Continued.*

Table S2. Oligosaccharides detected by MALDI-TOF MS in negative ionization mode after depolymerization of porphyran by β-porphyranase A. (only ions with intensity ≥1% of the relative abundance are reported).

dp	m/z		Tentative assignment
	experimental	theoretical	
2	421.10	421.07	[(L6S–G)-Na]$^-$
3	583.17	583.15	[(G)(L6S–G)-Na]$^-$
	597.14	597.13	[(G)(L6S–G)+CH_3-Na]$^-$
4	745.17	745.17	[(L–G)(L6S–G)-Na]$^-$
	759.19	759.19	[(L–G)(L6S–G)+CH_3-Na]$^-$
	847.12	847.11	[$(L6S–G)_2$-Na]$^-$
	861.14	861.13	[$(L6S–G)_2$+CH_3-Na]$^-$
	863.08	863.08	[$(L6S–G)_2$-2Na+K]$^-$
	877.10	877.10	[$(L6S–G)_2$+CH_3-2Na+K]$^-$
5	889.19	889.21	[(G)(LA–G)(L6S–G)-Na]$^-$
	903.22	903.23	[(G)(LA–G)(L6S–G)+CH_3-Na]$^-$
	917.23	917.24	[(G)(LA–G)(L6S–G)+2CH_3-Na]$^-$
6	1033.25	1033.26	[$(LA–G)_2$(L6S–G)-Na]$^-$
	1051.30	1051.31	[(LA–G)(L–G)(L6S–G)-Na]$^-$
	1065.27	1065.28	[(LA–G)$(L6S–G)_2$+CH_3-Na]$^-$
	1079.28	1079.30	[(LA–G)(L–G)(L6S–G)+2CH_3-Na]$^-$
	1153.20	1153.20	[(LA–G)$(L6S–G)_2$-Na]$^-$
	1167.21	1167.22	[(LA–G)$(L6S–G)_2$+CH_3-Na]$^-$
	1169.17	1169.18	[(LA–G)$(L6S–G)_2$-2Na+K]$^-$
	1183.19	1183.19	[(LA–G)$(L6S–G)_2$+CH_3-2Na+K]$^-$
	1197.20	1197.21	[(LA–G)$(L6S–G)_2$+2CH_3-2Na+K]$^-$
	1215.21	1215.22	[(L–G)$(L6S–G)_2$+2CH_3-2Na+K]$^-$
	1303.14	1303.14	[$(L6S–G)_3$+CH_3-2Na+K]$^-$
	1317.15	1317.16	[$(L6S–G)_3$+2CH_3-2Na+K]$^-$
	1333.12	1333.13	[$(L6S–G)_3$+2CH_3-3Na+2K]$^-$
8	1357.36	1357.36	[$(LA–G)_2$(L–G)(L6S–G)-Na]$^-$
	1371.37	1371.38	[$(LA–G)_2$(L–G)(L6S–G)+CH_3-Na]$^-$
	1385.40	1385.39	[$(LA–G)_2$(L–G)(L6S–G)+2CH_3-Na]$^-$
	1459.29	1459.30	[$(LA–G)_2$$(L6S–G)_2$-Na]$^-$
	1475.25	1475.27	[$(LA–G)_2$$(L6S–G)_2$-2Na+K]$^-$
	1489.27	1489.29	[$(LA–G)_2$$(L6S–G)_2$+$CH_3$-2Na+K]$^-$
	1503.30	1503.31	[$(LA–G)_2$$(L6S–G)_2$+2$CH_3$-2Na+K]$^-$
	1521.30	1521.32	[(LA–G)(L–G)$(L6S–G)_2$+2CH_3-2Na+K]$^-$
	1611.26	1611.28	[(L–G)$(L6S–G)_3$+CH_3-Na]$^-$
	1625.28	1625.29	[(L–G)$(L6S–G)_3$+2CH_3-Na]$^-$
	1639.28	1639.31	[(L–G)$(L6S–G)_3$+3CH_3-Na]$^-$
10	1663.44	1663.46	[$(LA–G)_3$(L–G)(L6S–G)-Na]$^-$
	1781.33	1781.37	[$(LA–G)_3$$(L6S–G)_2$-2Na+K]$^+$
	1795.32	1795.38	[$(LA–G)_3$$(L6S–G)_2$+$CH_3$-2Na+K]$^+$
	1917.33	1917.37	[(LA–G)(L–G)$(L6S–G)_3$+CH_3-Na]$^-$
	1931.34	1931.39	[(LA–G)(L–G)$(L6S–G)_3$+2CH_3-Na]$^-$
12	2087.42	2087.47	[$(LA–G)_4$$(L6S–G)_2$-2Na+K]$^+$
	2283.49	2283.52	[(LA–G)$(L–G)_2$$(L6S–G)_3$+4$CH_3$-Na]$^-$

Text S2. Sequencing of β-porphyranase A oligosaccharides using ESI-MS^n.

Each chromatographic fraction from the porphyran depolymerization by β-porphyranase A, has been further analyzed by electrospray negative ionization MS^n fragmentation. Isolation and fragmentation of the dp2 ion at *m/z* 421.0645 induced mainly the rupture of the glycosidic bond of the disaccharide as observed from the formation of the major ions at *m/z* 241.0019 and 259.0123 corresponding to 6-O-sulfate galactose (Figure S2A). Given the specificity of β-porphyranase A[1, 5] and the fact that a negative charge is usually maintained on the non-reducing end residue upon fragmentation,[6] these two ions were attributed to the non-reducing end fragments B_1 and C_1 respectively. A series of A_1 ions at *m/z* 198.9915 ($^{0,2}A_1$), 168.9810 ($^{0,3}A_1$) and 138.9706 ($^{0,4}A_1$) resulting from intra-cyclic cleavages ascertained the presence of a sulfate group at the C-6 position of the non-reducing end galactose. Overall, these MS/MS data indicated that the dp2 fraction was a monosulfated galactosyl-galactose L6S–G in full agreement with the typical building block depicted for porphyran.[1] This L6S–G disaccharide appeared as the limit product of the enzymatic depolymerization of porphyran by β-porphyranase A.

The ESI-MS^2 fragmentation of the disulfated tetrasaccharide detected as its di-charged ion $[M-2Na]^{2-}$ at *m/z* 412.0583, resulted in glycosidic bond cleavages leading to the non-reducing end monosaccharide B_1 (*m/z* 241.0013), disaccharides B_2 (*m/z* 403.0530) and C_2 (*m/z* 421.0636), and trisaccharides B_3^{2-} (*m/z* 322.0271) and C_3^{2-} (*m/z* 331.0323) ions, and to the reducing end trisaccharides Z_3 (*m/z* 565.1052) and Y_3 (*m/z* 583.1155). Two cross–ring cleavages were also observed, producing the fragment ions $^{1,4}A_4^{2-}$ (*m/z* 367.0427) and $^{0,2}A_3^{2-}$ at (*m/z* 301.0220) (Figure S2B). These data together with further MS^3 to MS^5 fragmentations (data not shown), led to the following porphyran tetrasaccharide sequence (L6S–G)–(L6S–G).

The second disulfated tetrasaccharide SEC sub-fraction described with a mass increment corresponding to a methyl group by MALDI-TOF MS was also submitted to ESI-MS^2 fragmentation, targeting its doubly charged ion $[M-2Na]^{2-}$ at *m/z* 419.0663. It yielded a series of non-reducing end

(B_1, B_2/C_2 and B_3^{2-}/C_3^{2-} at *m/z* 241.0015, 417.0689/435.0794, and 329.0350/338.0420, respectively) and reducing end (Z_3/Y_3 at *m/z* 579.1209/597.1315) fragment ions issued from glycosidic cleavages. Three cross-ring cleavages at *m/z* 507.1004, 374.0507 and 308.0300 attributed to $^{1,4}X_3/^{1,4}A_4^{2-}/^{0,2}A_3^{2-}$, respectively, were also detected (Figure S2C). As both non-methylated and methylated dp4 yielded identical B_1 but different B_2 and C_2 ions, we assume that the methyl group is on the second galactose residue from the non-reducing end. These data together with further MS^3 to MS^5 fragmentation in both negative and positive ionization (data not shown), led to the following methylated tetrasaccharide sequence (L6S–G6Me)–(L6S–G).

As regards the SEC dp6 sub-fraction assigned mainly to a non-methylated hexasaccharide, the ESI-MS^2 fragmentation of the disulfated hexasaccharide as its doubly charged ion $[M-2Na]^{2-}$ at *m/z* 565.1051 yielded a series of non-reducing end fragments (B_1, B_2/C_2, B_3/C_3, B_4/C_4 and B_5^{2-}/C_5^{2-} at *m/z* 241.0015, 403.0532/421.0637, 547.0948/565.1051, 709.1463/727.1567 and 475.0741/484.0792, respectively, and reducing end fragments (Z_5/Y_5 at *m/z* 871.1981/889.2082) issued from glycosidic cleavages. Several cross–ring cleavages were identified at *m/z* 454.0689, 520.0896, 535.0949, 769.1679 and 799.1772 attributed to $^{0,2}A_5^{2-}$, $^{1,4}A_6^{2-}$, $^{0,2}A_6^{2-}$, $^{2,4}A_5$ and $^{1,4}A_5$, respectively (Figure S2D). Other minor fragments at *m/z* 493.0845, 565.1051 and 583.1156 (Figure S2D) were also observed and attributed to the opening of the anhydro-bridges (+18 mass units). These data together with further MS^3 to MS^7 fragmentations (data not shown) led to the following porphyran hexasaccharide sequence (L6S–G)–(LA–G)–(L6S–G).

The ESI-MS spectrum of the second dp6 sub-fraction containing mostly methylaled species was dominated by two $[M-2Na]^{2-}$ ions at *m/z* 572.1131 and 579.1210 attributed to hexasaccharide with 1 and 2 methyl groups, respectively (data not shown). ESI-MS^2 of the ion at *m/z* 572.1131 yielded a series of no reducing end fragments B_1, B_4/C_4 and B_5^{2-}/C_5^{2-} at *m/z* 241.0015, 723.1620/741.1725 and 482.0820/491.0871, respectively, and reducing end fragments Z_5/Y_5 at *m/z* 885.2139/903.2240 issued from glycosidic cleavages. Several cross–ring cleavages were identified at *m/z* 461.0768, 527.0976, 542.1027 and 813.1930 attributed to $^{0,2}A_5^{2-}$, $^{1,4}A_6^{2-}$, $^{0,2}A_6^{2-}$ and $^{1,4}A_5$, respectively (Figure S2E). Except

$^{0,2}A_6^{2-}$, all these fragments unambiguously demonstrated that the methyl group is not located on the reducing end disaccharide. Further examination of the spectrum revealed additional series of ions resulting from glycosidic cleavage, and that were helpful to locate the methyl group. For example, B_2/C_2 ions at *m/z* 403.0532/421.0637 and B_3 ion at *m/z* 547.0950 (identical to those of a non-methylated dp6) strongly support the presence of a methyl group on the G unit of the internal LA-G disaccharide. However, other ions such as B_2 at *m/z* 417.0688, and B_3/C_3 at *m/z* 561.1105/579.1210 (underlined in Figure S2E) indicated that an additional dp6 species was present with a methyl group on the non-reducing end LA-G disaccharide. Therefore, these ion distributions unambiguously indicate that the methylated dp6 comprised two hexasaccharide isomers differing by the position of the methyl group. Further MS^{3-7} fragmentations (data not shown) allowed to decipher the complete sequence of two isomers: (L6S–G)–(LA–G6Me)–(L6S–G) and (L6S–G6Me)–(LA–G)–(L6S–G). Taking into account the intensity of various fragment ions specific of each isomer, we assume a ≈ 30/70 ratio for (L6S–G6Me)/(LA–G6Me). ESI-MS^2 of the dimethylated ion at *m/z* 579.1204 yielded the non-reducing end fragments B_1 (*m/z* 241.0013), B_2/C_2 (*m/z* 417.0637/435.0788), B_3/C_3 (*m/z* 561.1101/579.1204), B_4/C_4 (*m/z* 737.1768/755.1872) and B_5^{2-}/C_5^{2-} (*m/z* 489.0893/498.0946), and the reducing end fragments (Z_5/Y_5 at *m/z* 889.2287/917.2389) issued from glycosidic cleavages. There were accompanied by cross–ring cleavage ions at *m/z* 468.0842 ($^{0,2}A_5^{2-}$), 534.1049 ($^{1,4}A_6^{2-}$) and 827.2075 ($^{1,4}A_5$) (Figure S2F). All these MS^2 fragments indicated that the methyl groups were not located at the reducing end disaccharide. These results were completed by further fragmentations up to MS^7 that delineated the following sequence (L6S–G6Me)–(LA–G6Me)–(L6S–G) for this fourth hexasaccharide isomer contained in the dp6 fraction.

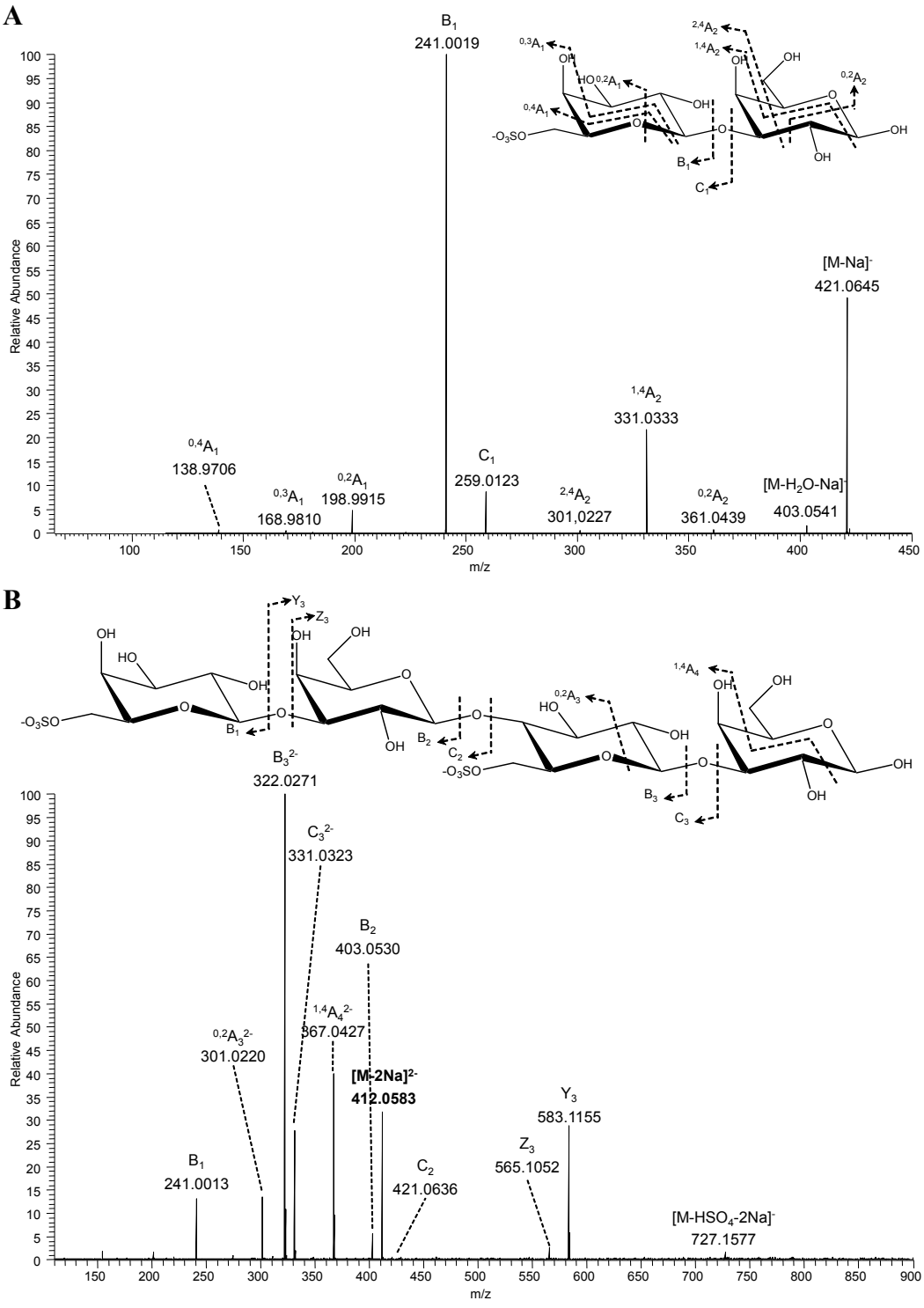

Figure S2. Negative ESI-MS/MS of purified porphyran oligosaccharide fractions produced by porphyranase A. Fragmentation of the most intense ion of the fractions (A) dp2 (m/z 421.0645), (B) dp4 (*m/z* 412.0583), (C) dp4-Me (*m/z* 419.0663), (D) dp6 (*m/z* 565.1051) and (E-F) dp6-Me (m/z 572.1131 and 579.1204 respectively). Fragments containing a methyl group at the non-reducing end were underlined.

C

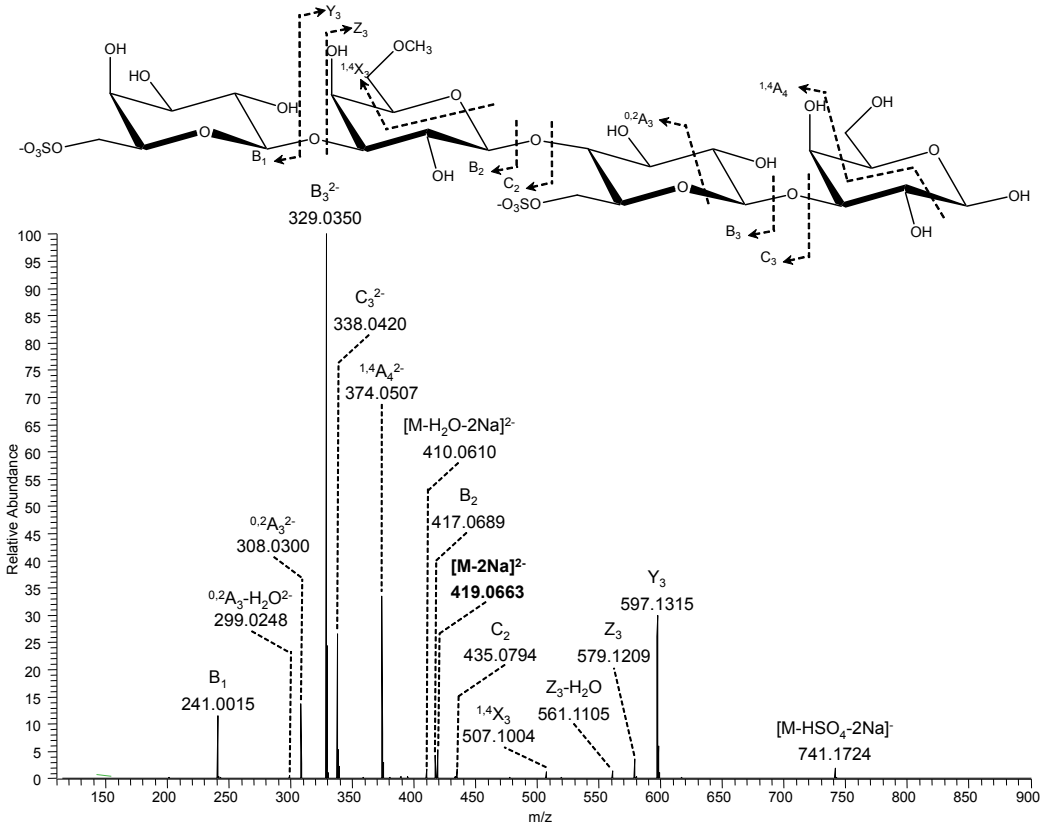

D

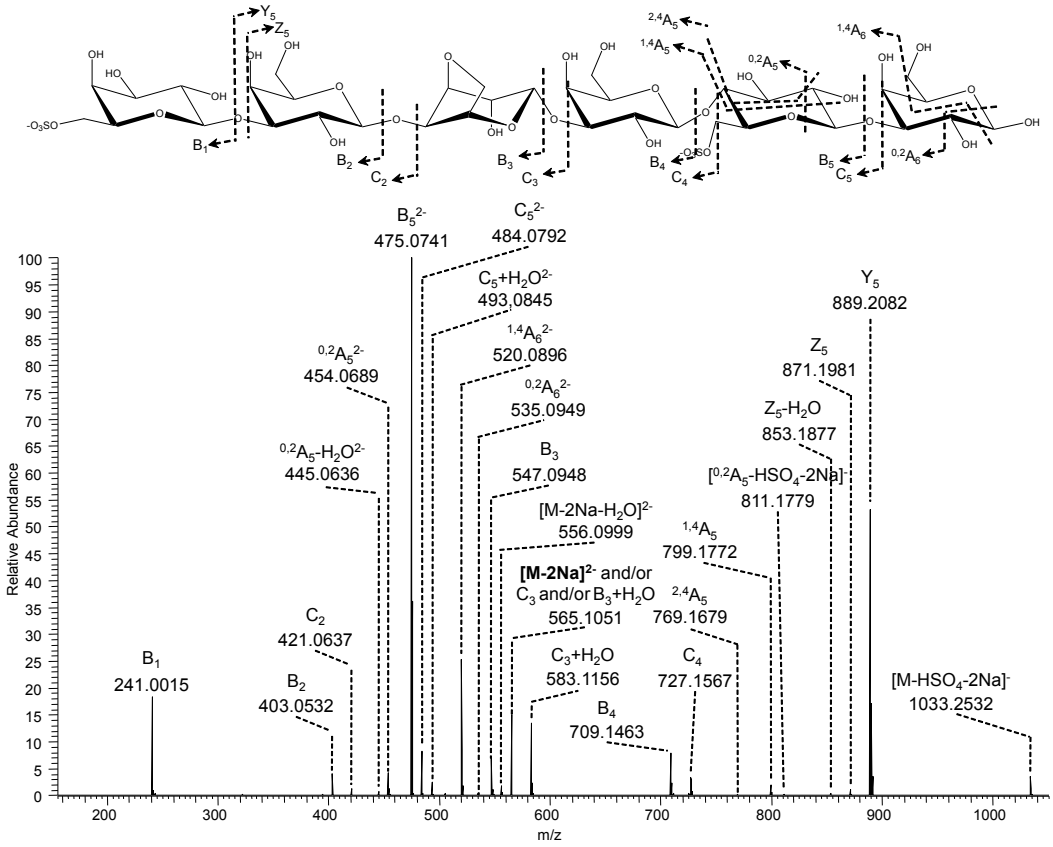

Figure 2. *Continued*.

E

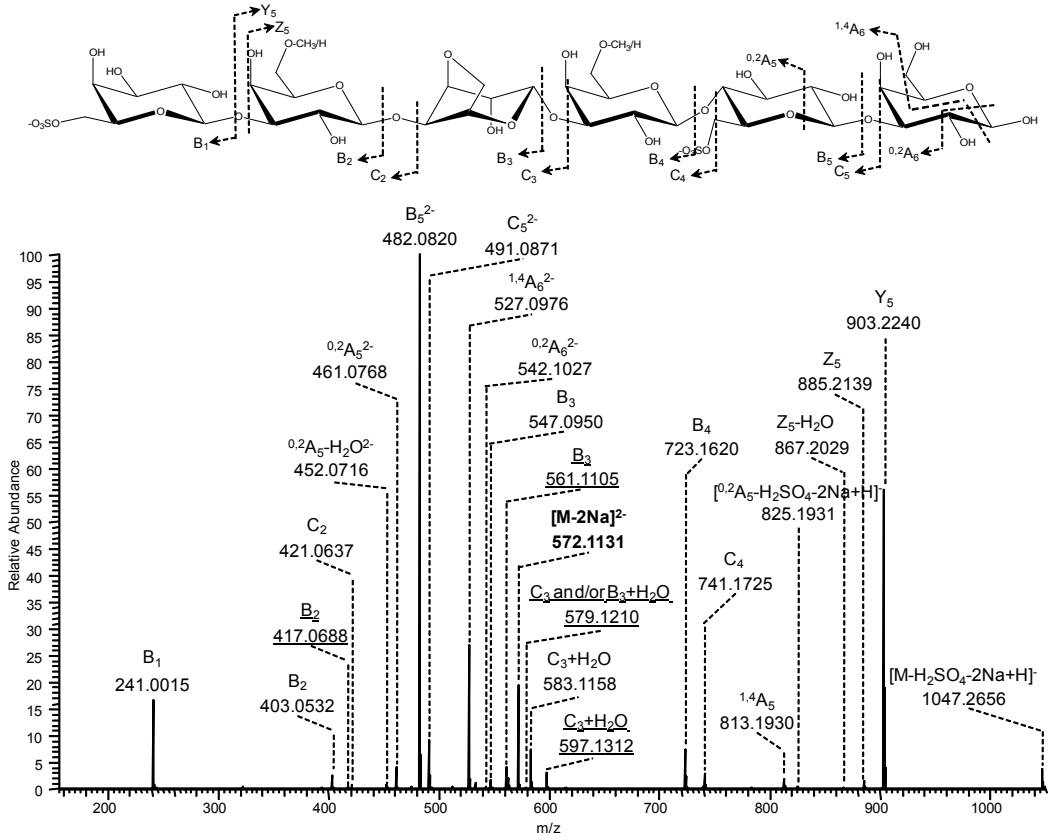

F

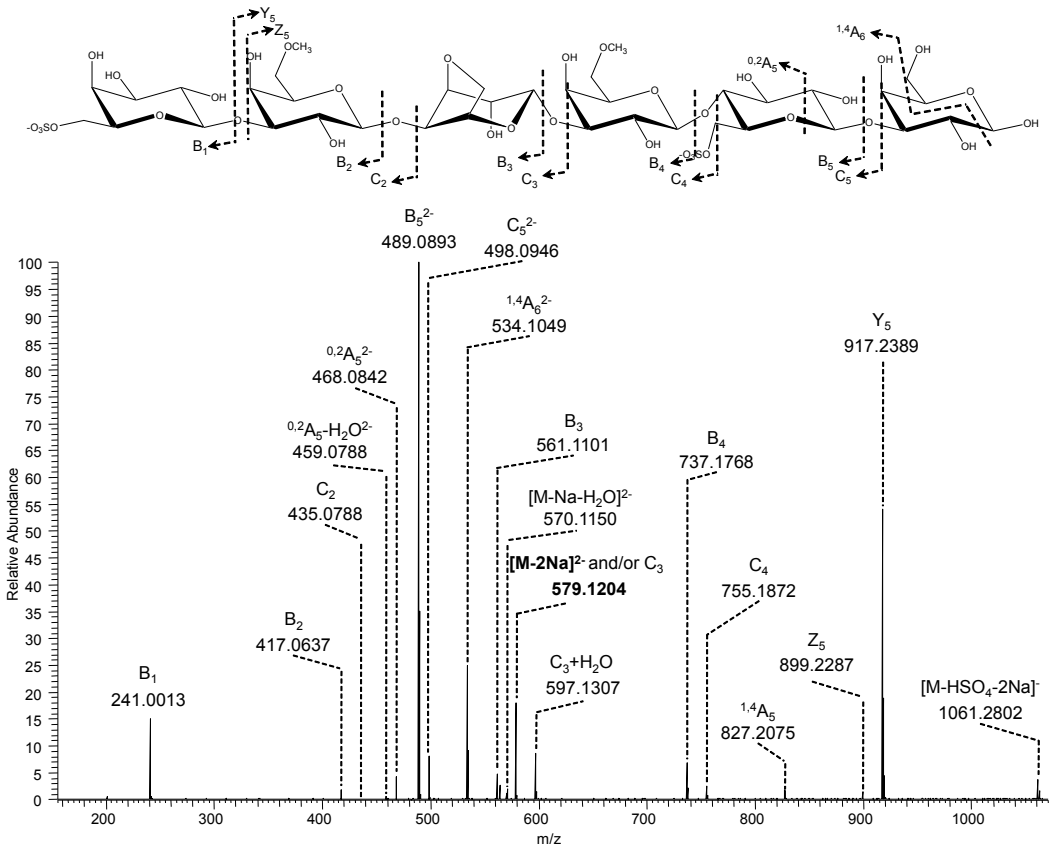

Figure 2. *Continued*.

REFERENCES

1. G. Correc, J.-H. Hehemann, M. Czjzek and W. Helbert, *Carbohyd. Polym.*, **2011**, 83.
2. C. Przybylski, F. Gonnet, D. Bonnaffé, Y. Hersant, H. Lortat-Jacob and R. Daniel, *Glycobiology*, **2010**, 20.
3. A. Seffouh, F. Milz, C. Przybylski, C. Laguri, A. Oosterhof, S. Bourcier, R. Sadir, E. Dutkowski, R. Daniel, T. H. van Kuppevelt, T. Dierks, H. Lortat-Jacob and R. R. Vivès, *FASEB J.*, **2013**, 27.
4. D. Ropartz, P.-E. Bodet, C. Przybylski, F. Gonnet, R. Daniel, M. Fer, W. Helbert, D. Bertrand, H. Rogniaux and 0., *Rapid Commun. Mass Spectrom.*, **2011**, 25.
5. J.-H. Hehemann, G. Correc, F. Thomas, T. Bernard, T. Barbeyron, M. Jam, W. Helbert, G. Michel and M. Czjzek, *J. Biol. Chem.* , **2012**, 287.
6. C. Przybylski, F. Gonnet, W. Buchmann and R. Daniel, *J. Mass Spectrom.*, **2012**, 47.